Accepted article. 2023 International Conference on Rehabilitation Robotics.

A Wearable Testbed for Studying Variable Transmission in Body-Powered Prosthetic Gripping

Andrew I.W. McPherson*, Michael E. Abbott, Weston White, Yuri Gloumakov, and Hannah S. Stuart*

***Abstract*— For those with upper limb absence, body-powered prostheses continue to be popular for many activities despite being an old technology; these devices can provide both inherent haptic feedback and mechanical robustness. Yet, they can also result in strain and fatigue. Body-powered prosthetic graspers typically consist of a simple lever providing a relatively constant transmission ratio between the input forces from the user's shoulder harness and the grip force of their prosthetic prehensor. In the field of robotic hand design, new continuously varying transmissions demonstrate particular promise in generating a wide range of grasping speeds without sacrificing grip strength. These benefits, if applied to shoulder-driven prosthetic grippers, have the potential to both reduce shoulder exertion and fatigue. This work presents the integration of a continuously variable transmission into a body-powered, voluntary close prosthetic testbed. We introduce the design and validate its performance in a benchtop experiment. We compare constant transmission conditions with a force-dependent, continually varying condition. The device is mounted on a prosthetic emulator for a preliminary wearable demonstration.**

I. Introduction

Despite many years of research, users of upper-limb prostheses remain unsatisfied with current solutions [1], [2]. Myoelectric devices are cosmetically appealing and allow for the actuation of dexterous hands capable of multiple grasps but lack the inherent haptic feedback present in normative grasping [3]. Body-powered (BP) prostheses, on the other hand, mechanically link the end-effector with the user's body. For example, shoulder-driven prosthesics utilize the contralateral shoulder to control the gripper through a Bowden cable and harness system, as shown in Fig. 1(a). This enables the instant transfer of haptic information such as force and motion between the user and the device in a control topology known as extended physiological proprioception (EPP) [4]. When compared to their myoelectric counterparts, BP prosthesis users exhibit a number of functional improvements, including faster completion times in both clinical [5] and at-home [6] settings, more accurate aperture sizing and stiffness discrimination [7], and more precise cursor tracing [8]. However, users continually rate excessive effort and related discomfort as key barriers to adoption [2].

A. Body-powered prosthesis transmissions

The cable transmissions used in voluntary closing (VC) BP prosthesis end-effectors typically consist of a simple lever arm, labeled L_c in Fig. 1(a), that directly actuates the gripper. This results in a fixed and inverse relationship between forces and positions related by the system's transmission ratio TR:

$$TR = \frac{F_g}{F_c} = \frac{\Delta x_c}{\Delta x_g} \tag{1}$$

where F_g and F_c represent the output grasp and input cable forces, respectively, and Δx_c and Δx_g represent the input cable excursion and output gripper travel, respectively. A device with a high TR augments its output force at the expense of larger ranges of motion required of the user to operate. This reduces the loads applied to the user's body, but the increased excursion can lead to awkward postures [11]. Reduced forces experienced at the shoulder with high TR devices can also lead to excessive grasping forces or crushing fragile objects [12]. On the other hand, lower TR devices result in responsive motion of the gripper but demand large forces from the user to grasp objects. The reduced positional demands have led this regime to be preferred for modern BP prostheses such as the TRS Grip 2S hook, which features a transmission ratio of $TR = 0.67$ [13]. However, the higher loads inherent to operating these devices cause discomfort and fatigue in users [14] and reduce users' pinch

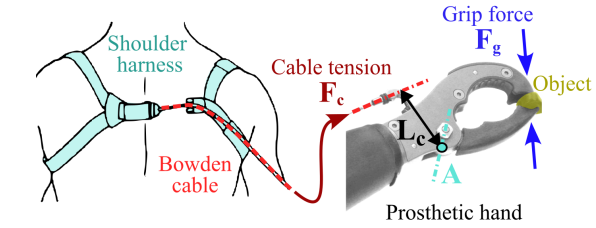

(a) Components of a shoulder-driven body-powered prosthesis.

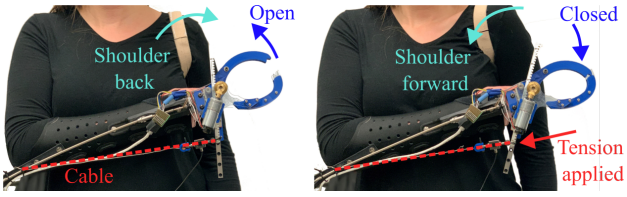

(b) Our wearable testbed.

Fig. 1. (a) Body powered prosthetic grippers commonly utilize a shoulder harness to apply Bowden cable tensions (F_c). This tension actuates a lever arm on the hand, labeled with the effective length L_c. This lever arm rotates about the axis at point A. Grip force (F_g) therefore results from shoulder-driven action as a function of L_c. Commercially available prostheses, like the one pictured here by TRS Inc., use a rigid or fixed-length lever arm. Images adapted from: (top-left) [9] and (top-right) [10]. (b) The proposed variable transmission is displayed alongside the gripper prototype in the bottom image. The user is seen exerting their shoulder to achieve a grasp closure. In this case, the lever arm is not extended since no object contact is made and no additional moment arm is needed to increase the grip force.

A.I.W. McPherson, M.E. Abbott, W. White, Y. Gloumakov, and H.S. Stuart are with the Embodied Dexterity Group, Dept. of Mechanical Engineering, University of California Berkeley, Berkeley, CA, USA.

* Corresponding authors email: drewmcpherson25@berkeley.edu, hstuart@berkeley.edu

There is a video supplement associated with this work.

force control [15].

B. Variable transmission for grasping

In an effort to mitigate the issues which follow from fixed-TR transmissions, researchers have developed variable transmissions for a variety of applications. In robotic manipulation, elastomeric tendon drums have been introduced that change shape under load to create a continuously variable transmission (CVT) [16], [17]. This results in a force-velocity relationship which varies with input force, where higher gripper velocities are realized at low input loads and higher grasp forces at high input loads for robotic hands. In another work, a cone-based CVT was used to change the interlocking relationships between shoulder rotation and elbow flexion with a single input from the control cable of a shoulder disarticulation BP prosthesis [18].

For cable-driven prosthetic grasping, a similar concept was applied with a discretely variable transmission integrated with a voluntary closing prehensor [11]. At minimal forces, a low transmission ratio mode enables fast action of the gripper until contact, which activates a toggle mechanism to flip the system into a high TR mode to amplify grasping force. Due to its bimodal nature, users reported difficulty in grasping soft objects such as towels or rolled newspapers because of the large range of motion required in the high TR mode [11].

These prior works focus primarily on device or transmission development with limited human subject testing of grasp performance improvement. To complement these works, controlled experimentation is also needed to evaluate the extent to which such variable transmissions affect human grasping performance and haptic understanding while operating BP prostheses. Our prior work with a desktop prosthesis simulation testbed has shown that a continuously variable transmission in body-powered prostheses allows for more successful grasping of objects with a wider variety of masses and stiffnesses than alternative transmission topologies in a grasping task [19]. The present work introduces a motorized wearable testbed device, pictured in Fig. 1(b) for emulating different fixed- and variable-transmission prostheses to assess the utility of CVTs across more realistic tasks.

C. Overview

In Sec. II, we discuss the kinematics of our prehensor, and define the relevant geometries and forces. We also present the design implementation, device functionality, and the control methods used in experiments. Sec. III shows the benchtop testbed used to characterize the device. Results presented in Sec. IV show how the implemented prehensor behaves in the expected manner during benchtop testing for both fixed TR and force-dependent TR conditions. In Sec. V we discuss the results and their implications, while Sec. VI summarizes the outcomes of this design study and motivates future efforts.

II. Design

We implement a varying TR in an upper-limb body-powered prosthesis by continuously adjusting the length of the input lever arm L_c as a function of cable tension. L_c can be either small ($L_{c,min}$) or large ($L_{c,max}$), as seen in Fig. 2(a) and (b) respectively. L_c is independent of the gripper aperture, shown for both the fully open and fully closed configurations. However, this architecture includes input cable forces which do not always act perpendicular to the lever arm, resulting in an additional geometric dependence on TR where transmission ratio varies with gripper motion and L_c.

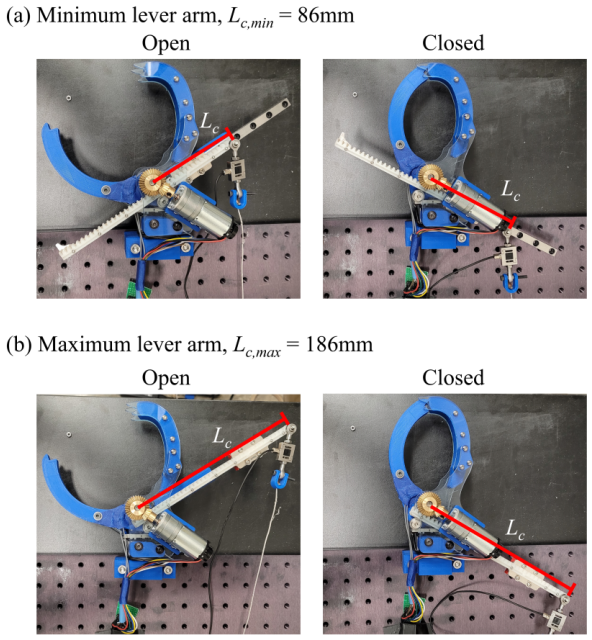

Fig. 2. Our proposed device includes a dynamically adjustable L_c, capable of increasing F_g without imposing increasingly fatigue-inducing shoulder-driven actuation. The TR is approximately 0.8 at its shortest (a), and approximately 1.7 at its longest $L_{c,max}$ (b).

A. Modeling

To better understand how the system behaves during operation, we model the device in terms of its geometry and forces (Fig. 3). Here, $\vec{F}_g$ corresponds to the grip force vector assumed to be perpendicular to the gripper arm $\vec{L}_g$, which originates at the center of rotation A and terminates at the end of the gripper arm G. The input cable force vector from the shoulder harness $\vec{F}_c$ acts along the line of action of the cable from the end of the lever arm at C to the cable origin point B. For clarity, we use scalar notation to denote magnitudes of vectors of the same name (e.g., $F_c = |\vec{F}_c|$) throughout this work.

Assuming static conditions in a moment balance about A, we can write the transmission ratio TR as a function of the lever arm length L_c and angle α between the lever arm direction and line of action of the cable force vector $\vec{F}_c$:

$$TR(L_c, \alpha) = \frac{F_g}{F_c} = \frac{L_c \sin\alpha}{L_g}. \quad (2)$$

Notably, α varies with changes to both lever arm length L_c and gripper angle θ, measured between the lever arm and the horizontal, which results in a changing effective moment arm of the cable force about the center of rotation at A.

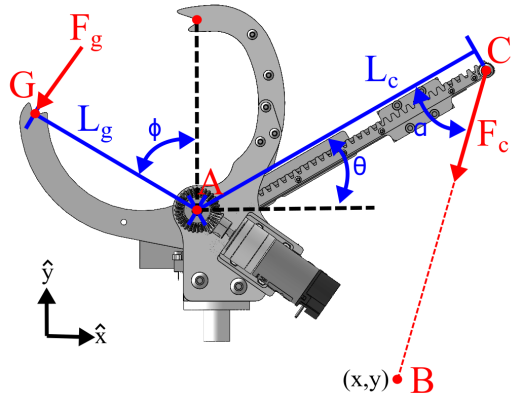

Fig. 3. Simple front view of prehensor CAD overlaid with force diagram showing the grip force F_g perpendicular to the gripper arm L_g and the shoulder cable force F_c acting at an angle θ relative to the lever arm L_c, both acting about point A. The gripper and lever arm are fixed such that they rotate as a single piece through a range of motion defined by the gripper angle θ. Point B represents the prosthesis cable origin point, beyond the frame of the figure.

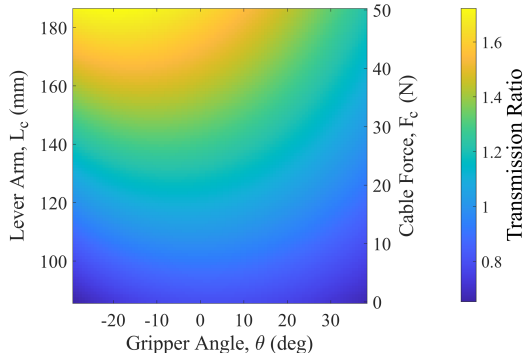

Fig. 4. Heatmap of theoretical transmission ratio as a function of gripper angle θ and lever arm length L_c. Assuming the controller $L_{c,var}$, input cable force F_c scales linearly with L_c. Gripper angle is measured in the counter-clockwise direction from the lever arm to the horizontal, where $38°$ represents the fully open state and $-29°$ represents the fully closed state.

To generate a variable transmission test condition, we define a desired lever arm length $L_{c,var}$ which varies linearly with the input cable force F_c:

$$L_{c,var}(F_c) = L_{c,min} + kF_c \tag{3}$$

where $L_{c,min}$ is the minimum lever arm length and k represents a linear scaling constant defined such that $L_{c,var}$ reaches the maximum lever arm length $L_{c,max}$ at an input cable force of 50N.

Fig. 4 shows model results demonstrating a transmission ratio varying based on the relative effects of both varying lever arm lengths and gripper motion. The TR ranges from 0.8 to 1.6 across these parameters. Changing L_c values appears to be the dominant factor in determining transmission ratio, with a 161% increase in TR across lever arm lengths in the fully closed state (i.e. $\theta = -29°$) and an 80.8% increase in the fully open configuration (i.e. $\theta = 38°$). At the minimum lever arm length $L_{c,min}$, we see a 22.0% change in transmission ratio across the full range of gripper motion and a 41.8% change in TR at the maximum lever arm length

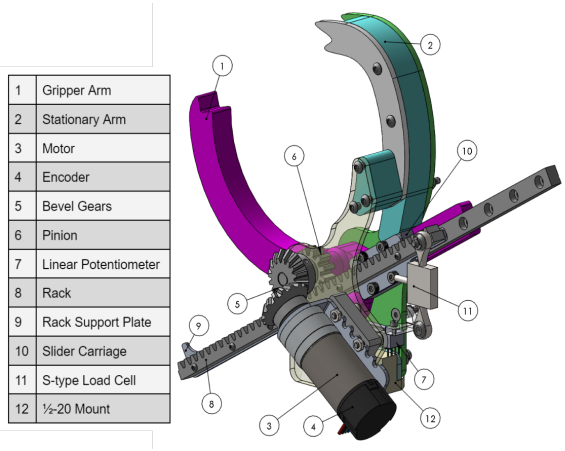

Fig. 5. Detailed CAD view of the prehensor and variable transmission components. The design is made up of three primary elements, the stationary arm, gipper arm, and variable lever arm assembly. Components are further described in sec II.

$L_{c,max}$. In the present work, we do not compensate for these geometric effects of gripper angle on TR.

B. Physical Implementation

Our prehensor implementation is inspired from the TRS Voluntary Close GRIP3 Prehensor, purchased with the TRS body-powered prosthesis simulator used in this work. The simulator was selected so the prototypes could be worn by able-bodied participants and rapidly evaluated by our team. The simulator includes a standard 1/2"-20 threaded prehensor receiver mounted to a low temperature, thermo-formable EXOS® forearm brace, designed to provide a comfortable fit for able-bodied participants. The gripper shape is roughly modeled after the TRS GRIP3, utilizing the threaded base for our prototypes so that it could interface with either the forearm simulator brace or standard prosthesis sockets.

The prehensor comprises 3D-printed PLA, laser-cut acrylic, aluminum, and off-the-shelf components. The stationary arm and gripping arm of the prehensor (parts 1-2) shown in Fig. 5 make up the basic function, with a central axis of rotation at A (Fig. 3). The stationary arm (part 2) gets rigidly mounted to the forearm brace and provides mounting for the remaining elements. A rack and pinion (parts 6, 8) is used to drive a linear bearing block (part 10) on a 150mm linear rail to vary L_c and thus the moment arm length. This linear slider railing is rigidly attached to the gripping arm (part 1) to transmit force from the cable to the gripper. An aluminum support plate (part 9) is mounted between the bearing block and rack to improve rigidity and maintain contact between the rack and pinion during large L_c travel.

The rack and pinion is actuated to change L_c by a 20.4:1 Metal Gearmotor 25Dx65L mm HP 12V with 48 CPR Encoder from Pololu. A momentary limit switch is also included near the bearing block position for $L_{c,min}$ to conduct absolute position homing. A pin in the gripper arm drives a 10kΩ linear potentiometer with a slot in the slide tab to measure angle ϕ position of the gripper. An S-type micro load cell (ATO-LC-S04) is attached at the end of the

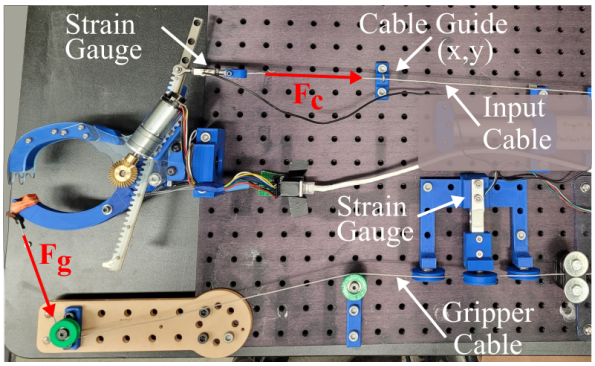

Fig. 6. The testbed used for benchtop validation of the prehensor with select tension sensors, cable guides and cable forces labeled. This image shows a grasping case of a small firm object simulated with a tension cable, thus the gripper is nearly closed in the $L_{c,min}$ case.

rack to measure tension in the input cable from the shoulder harness to implement control for $L_{c,var}$.

C. Control

The primary grasping motion is still achieved as with the traditional body-powered, voluntary close prehensor, through the motion of the shoulder. The supplemental active force-dependent mode $L_{c,var}$ uses the measured input cable force F_c to vary the TR. As the user grips an object with greater force, the moment arm extends by increasing L_c until the desired $L_{c,var}$ is reached. As a result, TR increases which in turn decreases the amount of force required by the user to apply an increased amount of grip strength.

We use cascaded motor commands to achieve the desired $L_{c,var}$, with a proportional force controller wrapped around a proportional-integral velocity controller. This is implemented on an Arduino Uno using a Pololu motor driver (VNH5019).

III. Validation Methods

Benchtop testing was performed first to validate the prehensor prototype achieves the desired transmission changes. This was done experimentally by mounting the prehensor horizontally to an optical breadboard with a custom in-line tension sensor and cable guides to measure cable force F_c and grip force F_g, as depicted in Fig. 6. For measuring F_g, we use a 10kg load cell (TAL220) strain gauge and SparkFun Qwiic Scale, NAU7802 amplifiers. The input (shoulder) cable was routed through a guide at a known location (x,y) to ensure consistent pull angles.

During experiments, the "input cable" was pulled slowly by hand from a fully open grasp angle ϕ_{max}. The "gripper cable" constrains the gripper to stop moving at an intermediate ϕ. The gripper cable length can therefore be adjusted to simulate different object sizes. We first test actuation forces up to $F_c = 50$N for a "firm" or high stiffness simulated object. Then, to simulate a "soft" or compliant object, the same gripper cable setup was used, but now in series with several rubber bands in parallel to allow for compliance. For the compliant object, F_c was increased until it either exceeded 50N and $L_c = L_{c,max}$, or until the prehensor was fully closed, whichever occurred first. Each object ("firm" and "soft") was grasped at least 10 times with the lever arm in each of three configurations: (1) the force varying lever arm $L_{c,var}$, (2) the shortest position $L_{c,min}$, and (3) longest position $L_{c,max}$.

IV. Results

A. Firm Object Grasping Results

From the data collected on the benchtop testbed for the firm simulated object, we can see that the cable force vs. grasp force plot for the three transmission cases match our expectations (Fig. 7a). The two constant transmission ratios $L_{c,min}$ and $L_{c,max}$ in red and gold, respectively, show a linear relationship. Note that the $L_{c,min}$ produces less maximum grip force by almost a factor of 2. The force-varying $L_{c,var}$ transmission data, in blue, illustrates the increasing mechanical advantage and therefore grip force as the cable force increases, transitioning from matching the $L_{c,min}$ grip force at low cable force to matching $L_{c,max}$ grip force at high cable force as anticipated. The maximum grasp force for $L_{c,max}$ and $L_{c,var}$ both reach 80 N. For comparison, the average male key pinch strength is 104 N and female is 73 N [20]. Everyday tasks often require less grip force, such as inserting a plug (31.4N) even under slippery conditions [21]. For all three cases, we observe hysteresis in the force curves, with the lower path occurring during the grasping phase and the upper values in the release phase.

Calculating the transmission ratio experimentally by dividing the grip force by cable force is shown in Fig. 7b. The two constant $L_{c,min}$ and $L_{c,max}$ modes have approximately horizontal lines, and thus have roughly constant TR at about 0.8 and 1.6, respectively. The force-varying $L_{c,var}$ mode transitions between these two TR levels as cable force increases. The grey shaded regions shown in Fig. 7b and 8b below are artifacts of the collected data and represent transition regions as contact begins to occur, where our calculation of TR will approach 0 as grip force goes to 0 both prior to contact and following release. Hysteresis, as well as a gently decreasing TR in the constant moment arm cases, is apparent in this plot. It is expected that these nonidealities arise from the compliance and flexing of the experimental testbed and friction points in the mechanism and cable routing.

Given the initial motivation of optimizing grip strength while reducing overall shoulder excursion, we also estimate this behavior in Fig. 7c. This estimate of cable excursion is performed using the measured values of L_c using the motor encoder and ϕ using the onboard linear potentiometer and the model in Fig 3. Here we can see $L_{c,min}$ contacts the object with less than half the excursion (60mm) required for $L_{c,max}$ (130mm), and requires less overall excursion. $L_{c,max}$ requires the same amount of shoulder excursion as $L_{c,min}$ for initial contact. The varying transmission $L_{c,var}$ requires less excursion (100mm) as compared with the $L_{c,max}$ case (150mm) to achieve the same maximum grip force. Given that the shoulder has limited range of motion, this difference could provide functional benefits to prosthesis users.

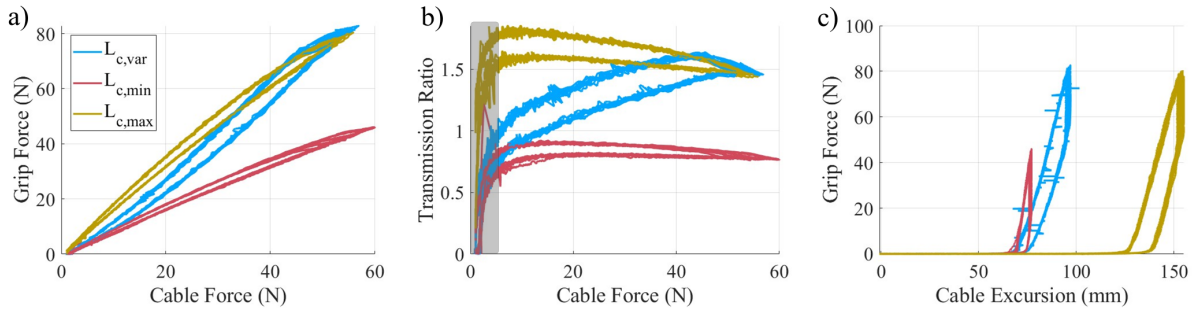

Fig. 7. Firm simulated object grasping results. The legend in plot a) is the same across plots b) and c). For all plots, $L_{c,var}$ shifts from the $L_{c,min}$ curve to the $L_{c,max}$ curve as the cable force increases, increasing its effective moment arm. In plots a) and b), the grip and cable forces travel counterclockwise as the cable is pulled and released due to hysteresis. In plot c) this is clockwise. a) In the static L_c conditions, grip force linearly changes with cable force, while $L_{c,var}$ transitions between them. b) Transmission ratio is generally constant for the static L_c conditions, however, below ∼5N of cable force, transmission ratios are undefined and the presented data is a result of data collection artifacts. c) Cable excursion is directly related to the length of the lever arm L_c and gripper angle.

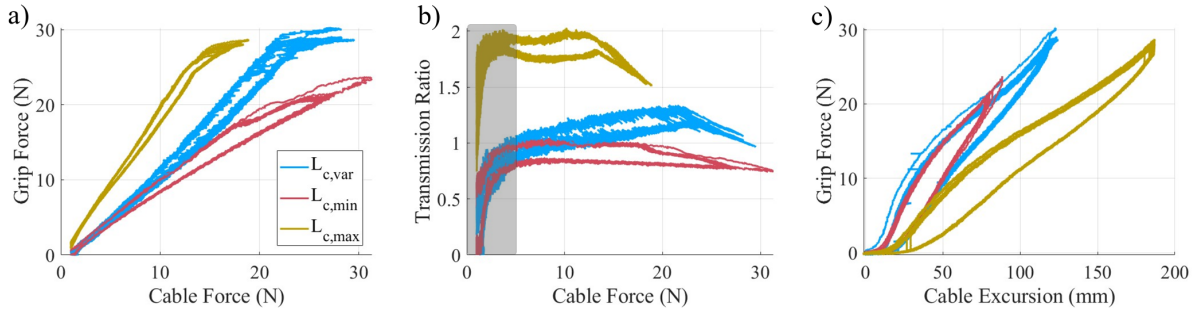

Fig. 8. Soft simulated object grasping results. The legend in plot a) is the same across plots b) and c). Much of the transmission behavior is the same as that of the previous firm object. However, the max forces are far lower as the gripper fully closed, making contact with the stationary arm due to the compliance of the object. Given this, $L_{c,var}$ did not transition all the way to $L_{c,max}$. Hysteresis can also be observed in all plots. Plot c) stands out as the most different from the firm case as the $L_{c,var}$ mode requires far less excursion than $L_{c,max}$ to reach the same max force despite both making contact at approximately the same cable position.

B. Soft Object Grasping Results

A second set of results for the soft object data is presented in Fig. 8. The behavior follows a similar trend as the firm case, with a few key differences. In Fig. 8a, the F_c versus F_g graph shows how we were unable to reach the full F_c input of 50N because the simulated object deformed to the point that the gripper was fully closed. This limited F_c range is reflected in Fig. 8b as well. Fig. 8c stands out for this soft object. Contact with the simulated object is made near 0mm of cable excursion with the gripper almost fully open for all three control cases. Yet, the $L_{c,max}$ case requires substantially more excursion (180mm) than in $L_{c,var}$ (120mm) to perform a grasp to the same grip force level. This demonstrates one of the advantages of the transmission's continuous nature, where previous discretely variable systems switch to a high TR mode (i.e. $L_{c,max}$) immediately upon contact regardless of object stiffness.

V. Discussion

The evaluation of this new body-powered prehensor testbed with integrated CVT demonstrates the ability to perform desired variable and fixed transmission functions in a programmable manner. This device shows the desired flexibility for future testing of a variety of transmission behaviors in human subjects, including continually varying schemes. The force plots in Fig. 7a and 8a illustrate how a greater grasping force can be achieved with less effort from the user in the $L_{c,max}$ and $L_{c,var}$ modes. This is reinforced in Fig. 7b and 8b by showing how the TR increases in the CVT $L_{c,var}$ mode from that of $L_{c,min}$ case to $L_{c,max}$ as cable force increases. In Fig. 7c and Fig. 8c, we demonstrate that the greater pinch force afforded with the longer lever in the $L_{c,var}$ case does not inherently necessitate the negative tradeoff of excessive excursion. All of this leads to improved behavior such that the user must only perform minimal shoulder motion for tasks requiring low F_g but can benefit from the greater TR as force requirements increase.

In future work, this testbed enables quick and efficient comparative testing between various continuously variable, discretely variable, or fixed transmissions in a manner that is wearable and relevant to realistic dexterous manipulation tasks. It could also allow for individualized testing of specific transmission types and parameters for different users. By incorporating the common threaded prehensor base and keeping all testbed components thereon, the custom prehensor can be tested by either normative subjects using the thermoformable EXOS® forearm brace or individuals with limb difference utilizing their own personalized sockets.

Upon completing all benchtop testing, the prehensor was connected to the TRS body-powered prosthetic simulator forearm brace for initial impressions on how it feels to grasp everyday objects, as shown in Fig. 1. This allowed

the authors to perform an initial test of fit and feel. An accompanying video shows demonstrations in supplementary materials. The device operated similarly to when it was operating in benchtop testing. The tested objects (one firm and one soft) were experienced as feeling relatively easy to grasp, while the variable transmission mode increased the feeling of grip security as compared to the fixed TR mode.

A potential source of fatigue in future human subjects experiments is the weight and weight distribution of the prehensor. The prehensor, not including the simulator brace, weighs 498g. For comparison, the fully passive TRS GRIP VC prehensor ranges from 278g to 451g [10], on the order of the human hand [22]. However, weight has consistently been cited as a concern for many prosthesis users [1], [23] likely in part due to muscle atrophy and weight distribution. Given the distal weight distribution of the current design, we see it as an intermediary testbed to inform later lightweight designs with more optimized transmissions and more proximal weight distribution to ease human subjects experience. We will also explore fully passive variable transmissions inspired by the outcomes discovered through this wearable testbed; the goal is to improve robustness and reduce the weight and complexity associated with an active device.

VI. Conclusion

This work shows the initial design and implementation of a motorized CVT in a wearable body-powered prosthesis prehensor. It is designed as a testbed for future study of optimal transmission control in human subjects. This study validated the performance of this motorized and body-powered device to match designed specification. By developing a mixed active/passive assistive device, we leverage the actuation power of the shoulder and thus maintain the benefits of haptic feedback in body-powered devices. At the same time, the motorized element allows for direct grip force to be manipulated through the CVT to reduce demands on the user. This work is one step towards the design of more capable and comfortable body-powered prosthetic grippers that reduce fatigue-inducing shoulder forces as well as excessive shoulder excursion.

ACKNOWLEDGMENT

Andrew McPherson is supported by Dolores Zohrab Liebmann Fellowship and the National Science Foundation Trainee Fellowship Grant No. DGE- 2125913. Michael Abbott was supported by the National Science Foundation Graduate Research Fellowship Program (award number DGE 1752814). This work is additionally supported by the University of California at Berkeley. The authors acknowledge the support of the members of the Embodied Dexterity Group.

References

[1] E. Biddiss, D. Beaton, and T. Chau, "Consumer design priorities for upper limb prosthetics," *Disability and Rehabilitation: Assistive Technology*, vol. 2, no. 6, pp. 346–357, Jan. 2007.

[2] E. A. Biddiss and T. T. Chau, "Upper limb prosthesis use and abandonment: A survey of the last 25 years," *Prosthetics and Orthotics International*, vol. 31, no. 3, pp. 236–257, Jan. 2007.

[3] S. L. Carey, D. J. Lura, and M. J. Highsmith, "Differences in myoelectric and body-powered upper-limb prostheses: Systematic literature review," *J of Rehabilitation Research and Development*, vol. 52, no. 3, pp. 247–262, 2015.

[4] D. Simpson, "The choice of control system for the multimovement prosthesis: Extended physiological proprioception (epp)," *The Control of Upper-extremity Prostheses and Orthoses*, pp. 146–150, 1974.

[5] D. Chappell, Z. Yang, H. W. Son, F. Bello, P. Kormushev, and N. Rojas, "Towards Instant Calibration in Myoelectric Prosthetic Hands: A Highly Data-Efficient Controller Based on the Wasserstein Distance," in *2022 Int. Conf. on Rehabilitation Robotics (ICORR)*, Jul. 2022, pp. 1–6.

[6] A. J. Spiers, J. Cochran, L. Resnik, and A. M. Dollar, "Quantifying Prosthetic and Intact Limb Use in Upper Limb Amputees via Egocentric Video: An Unsupervised, At-Home Study," *IEEE Trans. on Medical Robotics and Bionics*, vol. 3, no. 2, pp. 463–484, May 2021.

[7] M. A. Gonzalez, C. Lee, J. Kang, R. B. Gillespie, and D. H. Gates, "Getting a Grip on the Impact of Incidental Feedback From Body-Powered and Myoelectric Prostheses," *IEEE Trans. on Neural Systems and Rehabilitation Engineering*, vol. 29, pp. 1905–1912, 2021.

[8] J. A. Doubler and D. S. Childress, "An analysis of extended physiological proprioception as a prosthesis-control technique." *J of Rehabilitation Research and Development*, vol. 21, no. 1, pp. 5–18, 1984.

[9] J. F. Lehmann, "Orthotics for the wounded combatant," *Textbook of Military Medicine, Part IV. Rehabilitation of the Injured Combatant*, vol. 2, pp. 703–740, 1917.

[10] "Adult grip prehensors," https://www.trsprosthetics.com/product/adult-grip-prehensors/. Accessed: 2023-03-06.

[11] D. D. Frey and L. E. Carlson, "Technical note A body powered prehensor with variable mechanical advantage," *Prosthetics and Orthotics International*, vol. 18, no. 2, pp. 118–123, Jan. 1994.

[12] M. E. Abbott, J. D. Fajardo, H. Lim, and H. S. Stuart, "Kinesthetic feedback improves grasp performance in cable-driven prostheses," in *2021 IEEE Int. Conf. on Robotics and Automation (ICRA)*, May 2021, pp. 10 551–10 557.

[13] G. Smit and D. H. Plettenburg, "Efficiency of voluntary closing hand and hook prostheses," *Prosthetics and Orthotics International*, vol. 34, no. 4, pp. 411–427, Dec. 2010.

[14] M. Hichert, A. N. Vardy, and D. Plettenburg, "Fatigue-free operation of most body-powered prostheses not feasible for majority of users with trans-radial deficiency," *Prosthetics and Orthotics International*, vol. 42, no. 1, pp. 84–92, Feb. 2018.

[15] M. Hichert, D. A. Abbink, P. J. Kyberd, and D. H. Plettenburg, "High Cable Forces Deteriorate Pinch Force Control in Voluntary-Closing Body-Powered Prostheses," *PLoS ONE*, vol. 12, no. 1, Jan. 2017.

[16] K. Matsushita, S. Shikanai, and H. Yokoi, "Development of Drum CVT for a wire-driven robot hand," in *2009 Int. Conf. on Intelligent Robots and Systems*, Oct. 2009, pp. 2251–2256.

[17] K. W. O'Brien, P. A. Xu, D. J. Levine, C. A. Aubin, H.-J. Yang, M. F. Xiao, L. W. Wiesner, and R. F. Shepherd, "Elastomeric passive transmission for autonomous force-velocity adaptation applied to 3D-printed prosthetics," *Science Robotics*, vol. 3, no. 23, Oct. 2018.

[18] A. Kato, M. Hirabayashi, M. G. Fujie, and S. Sugano, "Variable Interlock Mechanism Joining Shoulder Rotation and Elbow Flexion for Body-Powered Upper Limb Prostheses," in *2018 World Automation Congress (WAC)*, Jun. 2018, pp. 1–5.

[19] M. E. Abbott, A. I. McPherson, W. O. Torres, K. Adachi, and H. S. Stuart, "Effect of variable transmission on body-powered prosthetic grasping," in *2022 Int. Conf. on Rehabilitation Robotics (ICORR)*, Jul. 2022, pp. 1–6.

[20] V. Mathiowetz, N. Kashman, G. Volland, K. Weber, M. Dowe, S. Rogers *et al.*, "Grip and pinch strength: normative data for adults," *Archives of Physical Medicine and Rehabilitation*, vol. 66, no. 2, pp. 69–74, 1985.

[21] N. Smaby, M. E. Johanson, B. Baker, D. E. Kenney, W. M. Murray, and V. R. Hentz, "Identification of key pinch forces required to complete functional tasks." *J of Rehabilitation Research & Development*, vol. 41, no. 2, 2004.

[22] P. De Leva, "Adjustments to zatsiorsky-seluyanov's segment inertia parameters," *J of Biomechanics*, vol. 29, no. 9, pp. 1223–1230, 1996.

[23] S. Salminger, H. Stino, L. H. Pichler, C. Gstoettner, A. Sturma, J. A. Mayer, M. Szivak, and O. C. Aszmann, "Current rates of prosthetic usage in upper-limb amputees–have innovations had an impact on device acceptance?" *Disability and Rehabilitation*, vol. 44, no. 14, pp. 3708–3713, 2022.